Biosensors and Bioelectronics 79 (2016) 15–21

Contents lists available at ScienceDirect

Biosensors and Bioelectronics

journal homepage: www.elsevier.com/locate/bios

A graphene oxide-based FRET sensor for rapid and specific detection of unfolded collagen fragments

Xiuxia Sun, Jun Fan, Yuping Zhang, Hongli Chen, Yongqing Zhao, Jianxi Xiao *

State Key Laboratory of Applied Organic Chemistry, Key Laboratory of Nonferrous Metal Chemistry and Resources Utilization of Gansu Province, College of Chemistry and Chemical Engineering, Lanzhou University, Lanzhou 730000, PR China

ARTICLE INFO

Article history:
Received 24 September 2015
Received in revised form
16 November 2015
Accepted 2 December 2015
Available online 4 December 2015

Keywords:
Collagen
FRET
Graphene oxide
Peptide
Biosensor

ABSTRACT

The unstructured collagen species plays a critical role in a variety of important biological processes as well as pathological conditions. In order to develop novel diagnosis and therapies for collagen-related diseases, it is essential to construct simple and efficient methods to detect unfolded collagen fragments. We therefore have designed a FITC-labeled collagen mimic triple helical peptide, whose adsorption on the surface of GO effectively quenches its fluorescence. The newly constructed GO/FITC–GPO complex specifically detects unstructured collagen fragments, but not fully folded triple helix species. The detection shows a clear preference for the collagen targets with complementary GPO-rich sequences. The conformation-sensitive, sequence-specific GO-based approach can be applied as an efficient biosensor for rapid detection of unfolded collagen fragments at nM level, and may have great potential in drug screening for inhibitors of unfolded collagen. It may provide a prototype to develop GO-based assays to detect other important unstructured proteins involved in diseases.

1. Introduction

The unfolded species of collagen generated during the collagen degradation process serve as important targets for novel diagnosis and therapies (Li and Yu, 2013). Collagen, the major structural component of connective tissues, provides a molecular scaffold that supports and protects the softer tissues for the human body. The degradation of collagen by proteolytic enzymes plays a critical role in many biological processes such as tissue development and regeneration, organ morphogenesis and wound healing (Brinckerhoff and Matrisian, 2002; Cawston et al., 1999; Fields, 2013). However, the excessive breakdown of collagen results in a variety of diseases including arthritis, chronic wounds and tumors (Sternlicht and Werb, 2001; Woessner, 1998; Riley et al., 1995). Extensive efforts have been performed to develop antibodies and peptides that can target these unstructured, degraded products of collagen for pharmaceutical purposes (Caravan et al., 2007; Mueller et al., 2009; Pernasetti et al., 2006; Xu et al., 2000). It is technically difficult to produce antibodies with high-specificities against collagen due to its highly repetitive (Gly-X-Y)n amino acid sequence (Chichester et al., 1991; Srinivas et al., 1994). A humanized monoclonal IgG1 antibody has been discovered to recognize denatured collagen but not native collagen (Pernasetti et al., 2006). A tumor-homing peptide that specifically binds to the fragments of Type IV Collagen produced by MMP-2 has been identified by phage display library screening (Mueller et al., 2009). These approaches are often tedious and time-consuming, and suffer from low specificity and binding affinity (Mueller et al., 2009; Pernasetti et al., 2006). Though much progress has been achieved, there is still a great need to develop simple and efficient methods to detect unfolded collagen fragments.

Fluorescence resonance energy transfer (FRET) is a powerful analytical technique for target detection due to its sensitivity, simplicity and reproducibility (Sapsford et al., 2006). Graphene oxide (GO), a one-atom-thick two-dimensional carbon material, has been widely used for biological applications, since it displays extraordinary characteristics including large surface area, facile surface modification, high-biocompatibility and good aqueous dispersibility (Novoselov et al., 2004; Kumar et al., 2015; Yang et al., 2010). Most notably, GO has been demonstrated as an efficient quencher for a variety of fluorophores via non-radioactive electronic excitation energy transfer from the fluorophore to GO, and its large adsorption cross section enables it as a superior candidate acceptor for FRET biosensors (Novoselov et al., 2004; Kumar et al., 2015; Yang et al., 2010). The noncovalent binding of GO with dye-labeled single strand DNA (ssDNA) has been utilized to develop assays for target DNAs, proteins and metal ions (Lu et al., 2009; Jang et al., 2010; Yang et al., 2013). More recently, fluorescent biosensors based on the GO-dye tagged peptide complex have been designed to monitor various peptide–protein

* Corresponding author.
E-mail address: xiaojx@lzu.edu.cn (J. Xiao).

http://dx.doi.org/10.1016/j.bios.2015.12.004
0956-5663/

interactions, protease activities and cancer cell surface biomarkers (Feng et al., 2011; Lu et al., 2011; Bianying et al., 2013). These studies provide valuable opportunities to understand the biological roles of the target proteins, while they are limited to well-structured proteins till present. It remains a great challenge to develop assays for unstructured proteins or protein fragments involved in pathological conditions.

Here, we report the design of a fluorescent sensor for unfolded collagen peptide fragments by taking the advantage of both the exceptional properties of GO and the easy formation of the GO-peptide complex. Collagen forms the unique structure of triple helix, which is similar to DNA double helix (Brodsky and Ramshaw, 1997). The hydrogen bonding between each component chain of both collagen and DNA drives the formation of the multiplex (Brodsky and Ramshaw, 1997). Hybridization of DNAs has been widely used to design GO-based fluorescent sensors to detect complementary single stranded DNA (Gao et al., 2014). It has been shown that when the collagen fragments with repetitive GPO amino acid sequences are in the unfolded, single-stranded form, they can bind to Type I collagen fibers as well as collagen films by annealing (Wang et al., 2005; He et al., 2012). Inspired by these results, we hypothesize that the hybridization between unfolded, single stranded collagen fragments and complementary collagen triple helix sequences may be utilized to design a GO-based fluorescent sensor (Scheme 1). The FITC-labeled collagen mimic triple helical peptide can be adsorbed on the surface of GO via π–π interactions and hydrophobic interactions. The close proximity of the GO to the FITC moiety efficiently quenches the fluorescence of FITC through energy transfer or electron-transfer processes (Lu et al., 2011). However, in the presence of target single stranded collagen fragments, the binding of collagen fragments with FITC-labeled peptide lead to desorption of the peptide from the surface of GO, therefore recovering the original fluorescence of the FITC-labeled peptide. We have demonstrated that the strategy using GO-peptide complex can be successfully applied to detect unstructured collagen fragments specifically.

2. Materials and methods

2.1. Materials

Graphite power of analytical grade was obtained from InnoChem Science & Technology Co., Ltd. (Beijing, China). All peptides were synthesized by Chinese Peptide Company (Hangzhou, China). These peptides were purified by HPLC and confirmed by mass spectrometry. Fluorescein isothiocyanate (FITC) was purchased from Aladdin (Shanghai, China). The dialysis tube (1 kDa membrane cut off) was purchased from Green Boyuan Biological & Technology Co., Ltd. (Beijing, China). All the reagents obtained from commercial sources were of analytical grade and were used without further purification. Ultrapure water was used to prepare all the solutions.

2.2. Instruments

FTIR spectra were obtained on a Nicolet NEXUS 670 infrared spectrophotometer (Madison, Wisconsin). TEM micrographs were recorded using a FEI TECNAIG^2 transmission electron microscope (Hillsborough, Oregon). Raman spectra were measured at room temperature on a Renishaw InVia Raman Microscope with an excitation laser at 632.8 nm (NCNST). The diffraction pattern of GO and graphite was characterized using an X-ray power diffraction meter (D/MAX-2400, Rigaku Co., Japan). Fluorescence measurements were carried out using a RF-5301PC fluorescence spectrometer (Shimadzu Instruments Ltd., Japan).

2.3. Preparation of graphene oxide (GO)

The preparation of GO was carried out following the modified Hummers method (Lu et al., 2011; Bhunia and Jana, 2011; Song et al., 2013; Nandi et al., 2012; Wu et al., 2011). Graphite (0.6 g) was added into 72 mL of concentrated H_2SO_4 (98%) and cooled to 0 °C. $KMnO_4$ (3.82 g) was then added gradually under stirring and the temperature of the mixture was kept at 10–15 °C. After the complete addition, the temperature of the mixture was raised to 35 °C and kept for 30 min. Next, 80 mL of ultrapure water was added to the brownish gray paste; and the solution was heated to 100 °C and left stirring for 30 min. The reaction was terminated by sequential addition of 120 mL ultrapure water and 3 mL 30% H_2O_2 solution and stirred for 10 min. The mixture was first washed with 5% HCl and then washed with water followed by centrifugation until the complete removal of SO_4^{2-}. Finally, the product was air-dried for 48 h at 50 °C. The GO solution was prepared in 10 mM PBS (pH 7.4) by sonication for 30 min.

2.4. Preparation of FITC-labeled peptides

Peptide CPO(GPO)$_8$G (1.0 mg) was dissolved in 2 mL 50 mM Na_2CO_3–$NaHCO_3$ buffer (pH 9.0, 140 mM NaCl). FITC (2.0 mg) was dissolved in 2 mL 50 mM carbonate buffer (pH 9.0, 140 mM NaCl). The peptide and FITC solutions were mixed (the molar ratio of peptide: FITC as 1:12) and foil-wrapped to avoid the loss of fluorescence. The mixture was stirred constantly at room temperature for 16 h to complete the reaction. Finally, the product was repeatedly dialyzed against 10 mM PBS buffer to remove excessive

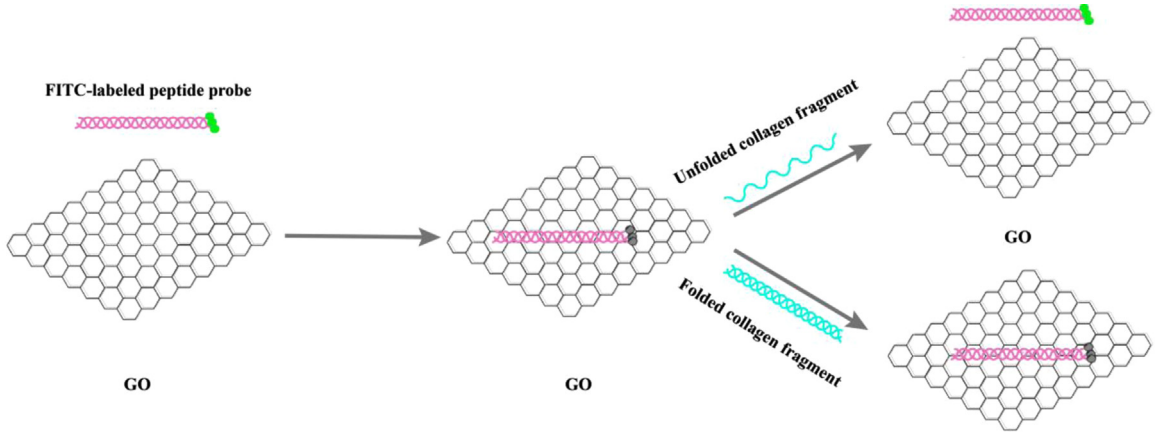

Scheme 1. Schematic Illustration of the concept of using a FITC-labeled triple helical peptide and GO complex to detect unfolded collagen fragments.

FITC. The fluorescence intensity of FITC in the dialysis buffer after exchange was monitored to assure the complete removal of FITC in the solution.

2.5. Monitoring the interaction of FITC labeled peptide with collagen mimic fragments

The FITC-labeled peptide $CPO(GPO)_8G$ (FITC–GPO) was dissolved in 10 mM PBS (pH 7.4) and serially diluted to obtain the desired concentration. Standard solutions of four unlabeled collagen mimic peptide fragments GPO (with amino acid sequence $CPO(GPO)_8G$), GPP (with amino acid sequence $DD(GPP)_{12}DD$), GPOALO (with amino acid sequence $(GPO)_5GPOALO(GPO)_5$), GERSEQ (with amino acid sequence $(GPO)_6GDRSER(GPO)_6$), were prepared by serial dilution using 10 mM PBS buffer, pH 7.4. The labeled peptide FITC–GPO (100 nM) was mixed with GO prior to the addition of target collagen mimic fragments. Then a range of collagen fragments with final concentrations (0–1100 nM) were added to the GO/FITC–GPO solution. The fluorescence of the mixture GO/FITC–GPO/collagen fragments was monitored.

3. Results and discussion

3.1. Characterization of GO

The synthesized GO was characterized by XRD, Raman, FTIR and TEM techniques (Fig. 1). The XRD patterns of GO and graphite were compared (Fig. 1A). The single intense peak for GO and graphite was at 2θ of 11.5° and 26.5°, respectively (Fig. 1A). The shift of the peak resulted from the larger interlay space of GO as compared with graphite, which was due to the introduction of oxygenated functional groups on carbon sheets. The Raman spectra of GO and graphite were also compared (Fig. 1B). The Raman spectrum of GO showed a strong peak assigned to the vibration of sp^2 – bonded carbon atoms at 1593 cm^{-1} (G band) and another well-documented strong peak assigned to the vibration of carbon atoms with dangling bonds at 1334 cm^{-1} (D band). In contrast, the Raman spectrum of graphite showed very weak peaks assigned to the D and G bands (Fig. 1B). The difference in the Raman spectra of GO and graphite may indicate the formation of some sp^3 – carbon atoms in GO, which was consistent with earlier reports (Lu et al., 2011; Sabale et al., 2014; Liu et al., 2012).

As illustrated in Fig. 1C, the GO showed intense FTIR peaks at 3428 cm^{-1} (O–H bond), 1730 cm^{-1} (C=O bond), 1622 cm^{-1} (the

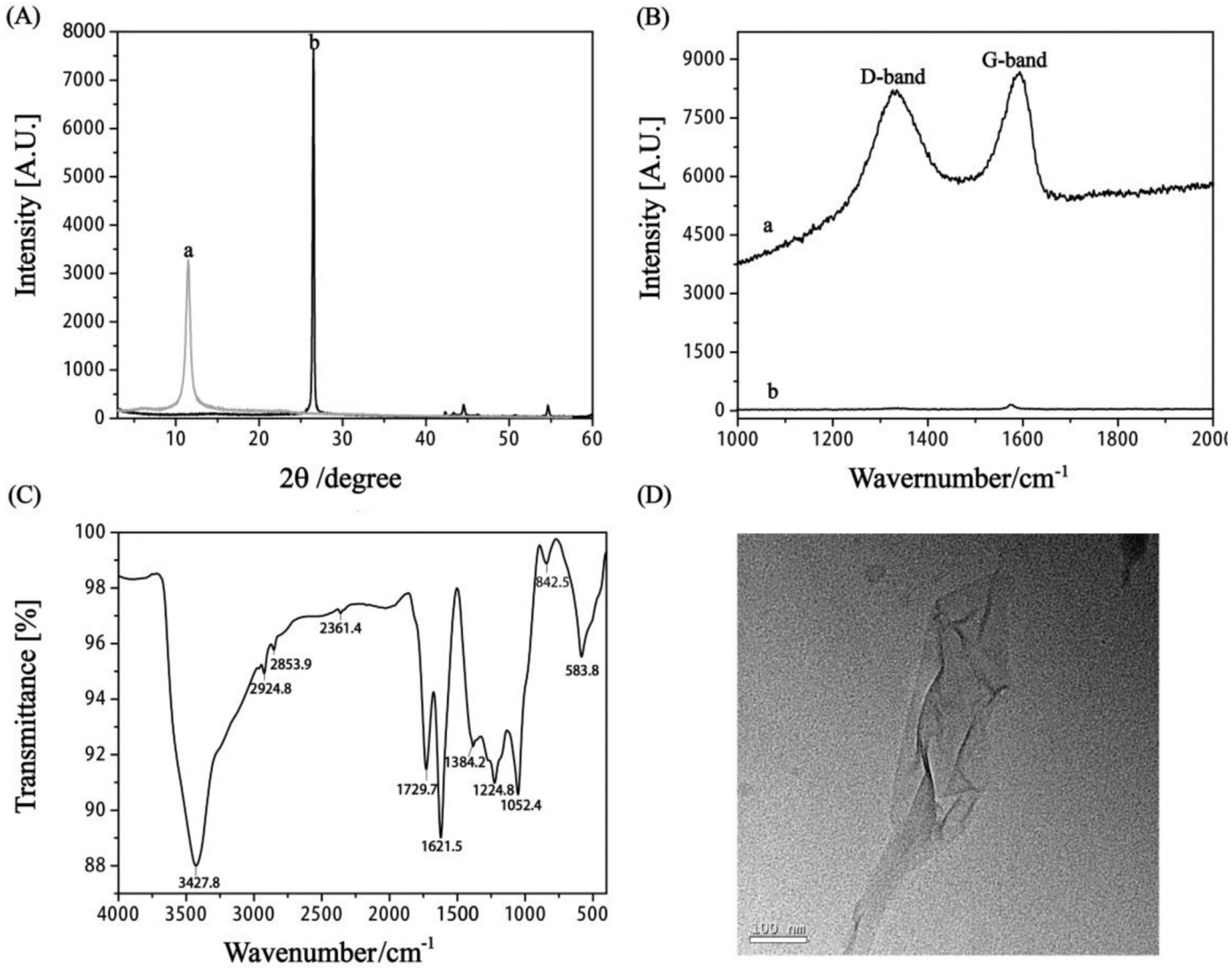

Fig. 1. Characterization of GO. (A) XRD patterns of GO (a) and graphite (b). (B) Raman spectra of GO (a) and graphite (b). (C) FTIR spectra of GO. (D) TEM image of GO.

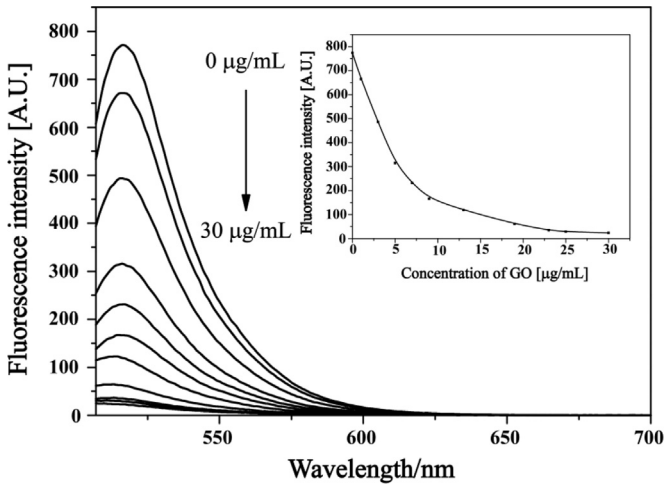

Fig. 2. The fluorescence quenching of FITC–GPO by various concentrations of GO. The fluorescence emission spectra were measured for FITC–GPO in the presence of various concentrations of GO (0, 1, 3, 5, 7, 9, 13, 19, 23, 25, and 30 μg/mL). Inset: the fluorescence intensity monitored at 517 nm as a function of GO concentration.

bonds of the unoxidized graphitic skeletal domains), 1225 cm^{-1} (C–OH bond), and 1052 cm^{-1} (C–O bond). The FTIR spectrum represented the characteristic vibrations of GO and matched well with that reported previously (Fig. 1C) (Lu et al., 2011; Liu et al., 2012). The TEM image displayed a typical layered structure of GO and agreed well with earlier studies (Fig. 1D) (Nandi et al., 2012; Sabale et al., 2014; Liu et al., 2012). The significant difference in the XRD and Raman spectra between GO and graphite as well as characteristic FTIR and TEM graphs of GO clearly indicated the successful synthesis of GO.

3.2. The fluorescence quenching of FITC–GPO by GO

The fluorescence emission spectra were measured for FITC–GPO in the presence of various concentrations of GO (0–30 μg/mL) (Fig. 2). The FITC labeled peptide FITC–GPO alone showed strong fluorescence at 517 nm (Fig. 2). With the addition of GO, the fluorescence intensity of FITC–GPO was significantly decreased. When the concentration of GO reached 30 μg/mL, the fluorescence of FITC–GPO was almost completely quenched. The quenching efficiency of the GO was estimated to be 97%. The high quenching efficiency would assure better sensitivity and a broader dynamic range for target detection.

3.3. Monitoring the interactions of FITC–GPO and collagen peptide fragment GPO

The fluorescence emission spectra were measured for the GO/FITC–GPO complex in the presence of various concentrations of collagen peptide fragment GPO (with amino acid sequence CPO $(GPO)_8G$) (Fig. 3A). Peptide GPO was chosen to restore the fluorescence of the GO/FITC–GPO complex as earlier studies suggested that the peptide with a similar GPO sequence could hybridize with Type I collagen when it was in the unfolded form (He et al., 2012). The collagen peptide fragment GPO was heated to 80 °C (which was much above its melting temperature) for 20 min to make sure that the peptide was completely unfolded. With the addition of unfolded GPO, a significant enhancement of the fluorescence was observed, suggesting that the competitive binding of the GPO with GO for FITC–GPO lead to the desorption of FITC–GPO from the surface of GO (Fig. 3A). When the concentration of the unfolded GPO was increased, the fluorescence intensity of the GO/FITC–GPO complex was gradually increased (Fig. 3A). Furthermore, a linear relationship between the concentration of the unfolded GPO and the change of the fluorescence intensity was observed ($R^2=0.99$) (Fig. 3A). The GO/FITC–GPO system allowed the accurate detection of unfolded GPO at a concentration as low as 10 nM, which was much lower than the hybridization conditions (50 μM for the probe peptide) reported in earlier studies (Wang et al., 2005).

To investigate if the fluorescence restoration capability of GPO was conformation-dependent, the fluorescence emission spectra was measured for the GO/FITC–GPO complex in the presence of fully folded GPO (Fig. 4A). The GPO solution was equilibrated at 4 °C for 48 h to make sure the triple helix formation prior to the addition. With the addition of 500 nM fully folded GPO, the fluorescence was only weakly increased from 30.3 to 45.3, while the same amount of unfolded GPO resulted in a significant enhancement from 25.4 to 147.4 (Fig. 4B). It indicated that the GO/FITC–GPO system was conformation-dependent, and it could only detect unfolded GPO, but not folded GPO.

3.4. Monitoring the interactions of FITC–GPO and collagen peptide fragment GPOALO

To investigate if the GO/FITC–GPO system was sequence-

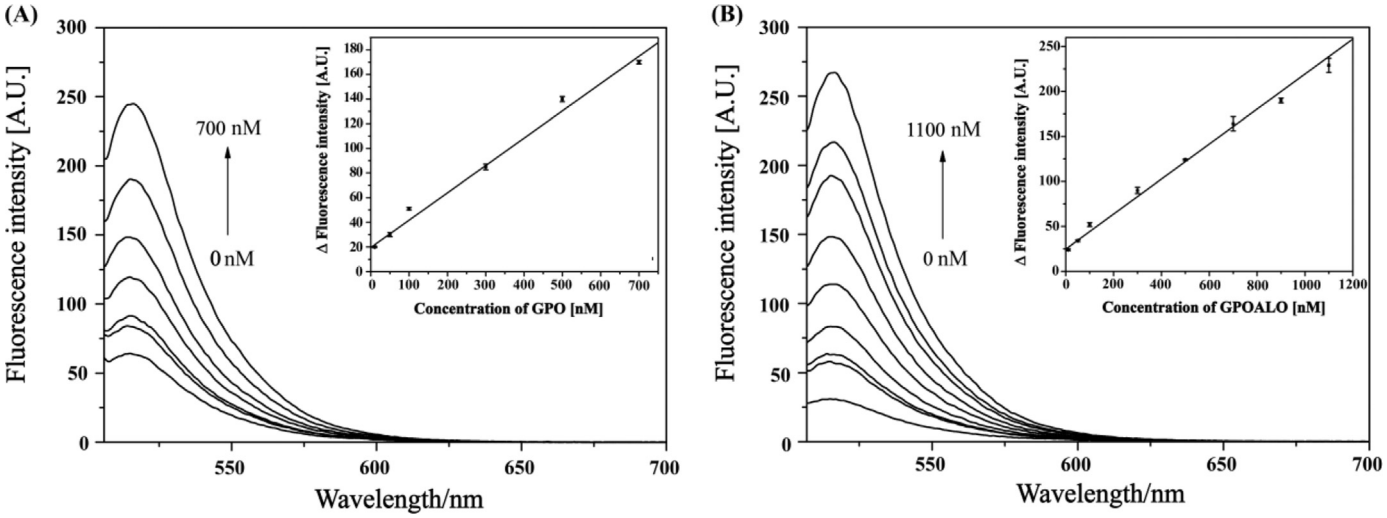

Fig. 3. The linear fluorescence restoration of the GO/FITC–GPO complex by the addition of unfolded collagen fragments GPO (A) and GPOALO (B). The fluorescence emission spectra were measured for the GO/FITC–GPO complex in the presence of various concentrations of GPO (0, 10, 50, 100, 300, 500, and 700 nM) or GPOALO (0, 10, 50, 100, 300, 500, 700, 900, and 1100 nM). Inset: the changes of the fluorescence intensity monitored at 517 nm as a function of the concentration of unfolded GPO or GPOALO.

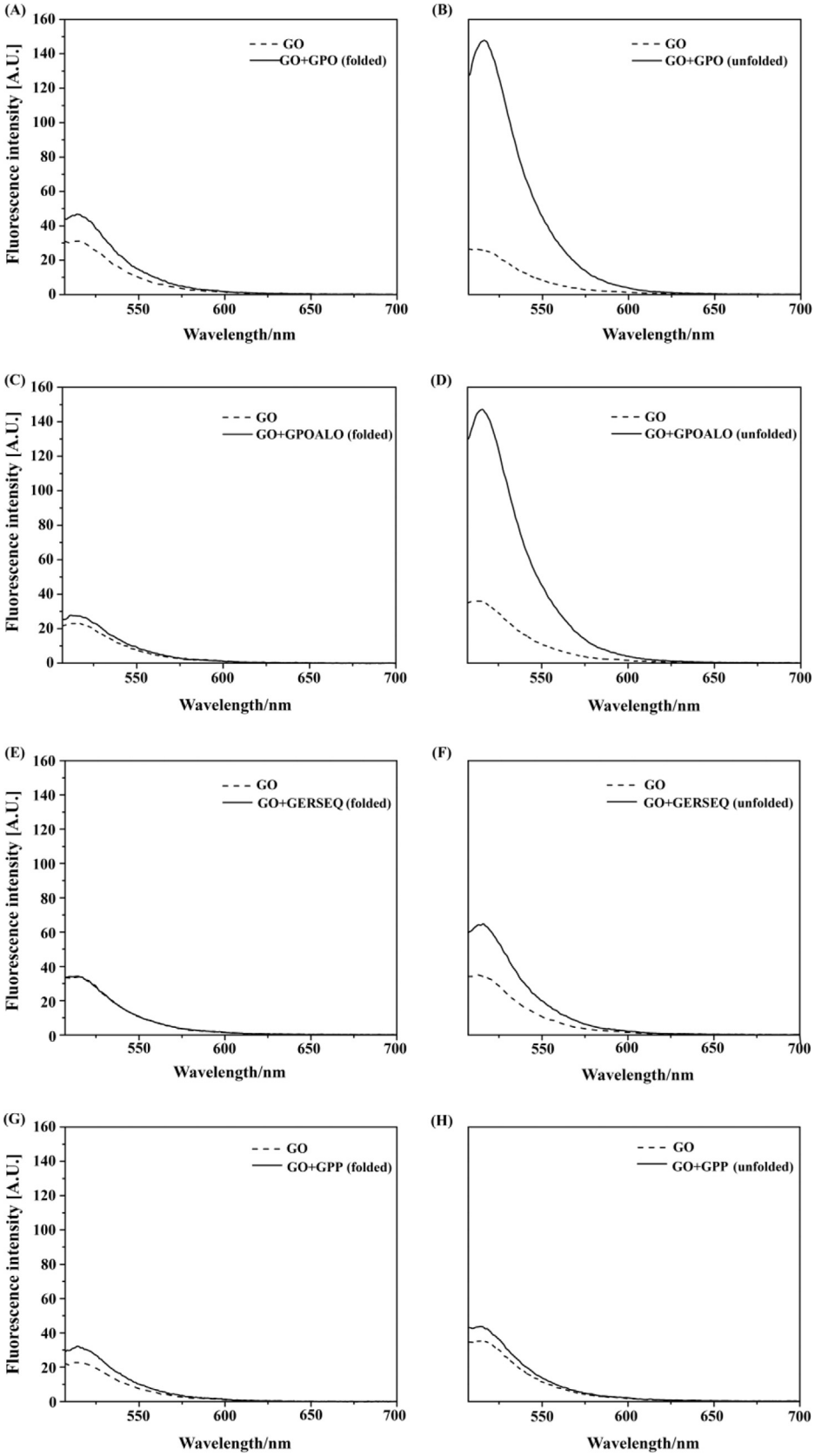

Fig. 4. The fluorescence restoration of the GO/FITC–GPO complex by fully folded triple helical collagen fragments (A, C, E, G) and corresponding unfolded collagen fragments (B, D, F, H). The fluorescence intensity of the GO/FITC–GPO complex was measured in the absence of collagen fragments (dashed) and in the presence of 500 nM collagen fragments (solid). The addition of fully folded GPO (A), GPOALO (C), GERSEQ (E) or GPP (G) could not restore the fluorescence of the GO/FITC–GPO complex. The addition of unfolded GPO (B) or GPOALO (D) could significantly restore the fluorescence of the GO/FITC–GPO complex, while the addition of unfolded GERSEQ (F) and GPP (H) led to small or insignificant fluorescence restoration, respectively.

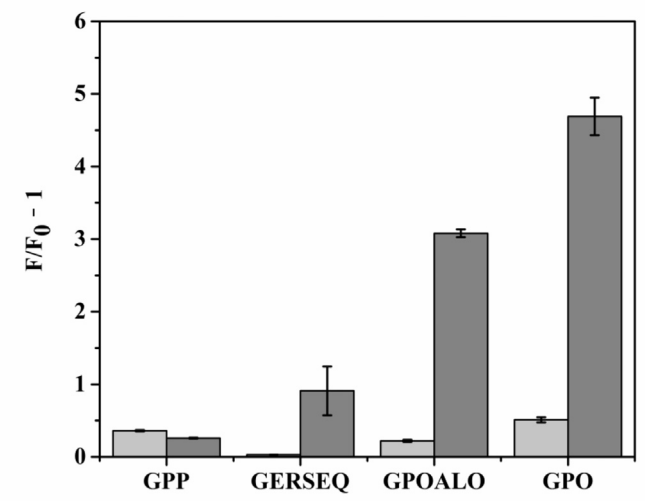

Fig. 5. The conformational and sequential dependence of the fluorescence restoration of the GO/FITC–GPO complex by collagen fragments. The changes of the fluorescence intensity (F/F_0-1) of the GO/FITC–GPO complex were calculated for different collagen fragments. F and F_0 were fluorescence intensities measured at 517 nm in the presence and absence of collagen fragments, respectively. The collagen fragments were in the fully folded state (gray) as well as the unfolded form (black). The fluorescence restoration of the system required the target to be in the unfolded form, while the restoration level was sequence-specific.

specific, the fluorescence emission spectra were measured with the addition of another collagen peptide fragment GPOALO (with amino acid sequence $(GPO)_5$ GPOALO$(GPO)_5$) (Fig. 3B). Compared with peptide GPO, the major modification of peptide GPOALO was changing the middle triplet GPO to ALO. With the addition of unfolded GPOALO, the fluorescence intensity of the GO/FITC–GPO complex was gradually increased (Fig. 3B). A linear relationship between the concentration of the unfolded GPOALO and the change of the fluorescence intensity was also observed ($R^2=0.99$) (Fig. 3B). Similarly with peptide GPO, the addition of 500 nM fully folded GPOALO only led to very weak increase of the fluorescence from 23.1 to 27.3, while the same amount of unfolded GPOALO resulted in a much larger enhancement from 34.9 to 145.3 (Fig. 4C and D). It indicated that the GO/FITC–GPO system was conformation-dependent, and it could only detect unfolded GPOALO, but not folded GPOALO.

3.5. Monitoring the interactions of FITC–GPO and collagen peptide fragments GERSEQ and GPP

The fluorescence restoration of the GO/FITC–GPO complex was further investigated using more collagen fragments GERSEQ and GPP to elucidate the sequential dependence (Fig. 4E–H). Compared with peptide GPO, the major modification of peptide GERSEQ was changing two middle triplets GPOGPO to GERSEQ, while peptide GPP changed all GPO triplets to GPP. For peptide fragment GERSEQ, the addition of 500 nM fully folded form did not affect the fluorescence intensity, while the same amount of unfolded form resulted in a small enhancement from 34.1 to 63.4 (Fig. 4E and F). For peptide fragment GPP, in contrast, both the addition of fully folded and unfolded form resulted in a tiny increase in the fluorescence (Fig. 4G and H). It indicated that the GO/FITC–GPO system was dependent on conformation as well as sequence.

3.6. Conformation and sequence selectivity of the GO/FITC–GPO platform

The fluorescence restoration capability of the four collagen fragments on the GO/FITC–GPO platform was compared (Fig. 5). The changes of the fluorescence intensity (F/F_0-1) were calculated to facilitate the comparison, where F_0 and F were the fluorescence intensities before and after the addition of the collagen fragments, respectively. First, the fluorescence restoration capability of the fully folded state (gray) was compared with that of the unfolded form (black) (Fig. 5). It was obvious that some unfolded peptides resulted in strong fluorescence restoration, while the folded state for all the four collagen fragments led to little fluorescence restoration. The results clearly demonstrated that the GO-based platform could specifically detect unfolded collagen species, but not folded collagen species.

The fluorescence restoration capability was further compared among the four collagen fragments in the unfolded form (Fig. 5). The restoration capability was in the order of GPP < GERSEQ < GPOALO < GPO, suggesting that the GPO-rich sequence was preferred by the GO/FITC–GPO system. The GPO triplet is the most stabilizing sequence for the triple helix structure, therefore, the complementary GPO sequence of the target peptide likely results in high binding affinity with the probe peptide, leading to the recovery of the fluorescence. While the sequence becomes more and more deviated from the GPO triplet environment, the collagen fragment probably possesses less binding affinity with the probe peptide, thus resulting in decreased restoration capability. To conclude, this novel GO-based assay shows a clear preference for GPO-rich sequences, while the restoration level is sequence-specific.

4. Conclusions

The unstructured collagen species plays a critical role in a variety of important biological processes as well as pathological conditions. Current collagen assays mainly using monoclonal antibodies suffer from tedious procedures, low specificity and binding affinity. In order to develop novel diagnosis and therapies for collagen-related diseases, it is essential to construct simple and efficient methods to detect unfolded collagen fragments. We therefore have successfully constructed a FITC-labeled collagen mimic triple helical peptide, whose adsorption on the surface of GO effectively quenches its fluorescence.

The newly developed GO/FITC–GPO complex provides a sensing platform that can specifically detect unstructured collagen fragments, but not fully folded collagen species. In addition, the platform shows a clear preference for the collagen targets with complementary GPO-rich sequences. The conformation-sensitive, sequence-specific GO-based approach can be applied as an efficient biosensor for rapid detection of unfolded collagen fragments at nM level, and may have great potential in drug screening for inhibitors of unfolded collagen. What is more, it may provide a prototype to develop GO-based assays to detect other important unstructured proteins involved in diseases.

Acknowledgments

This work was supported by grants from the National Natural Science Foundation of China (Grant no. 21305056) and the Fundamental Research Funds for the Central Universities (Grant no. lzujbky-2014-73).

References

Li, Y., Yu, S.M., 2013. Curr. Opin. Chem. Biol. 17, 968–975.
Brinckerhoff, C.E., Matrisian, L.M., 2002. Nat. Rev. 3, 207–214.

Cawston, T., Billington, C., Cleaver, C., Elliott, S., Hui, W., Koshy, P., Shingleton, B., Rowan, A., 1999. Ann. N. Y. Acad. Sci. 878, 120–129.
Fields, G.B., 2013. J. Biol. Chem. 288, 8785–8793.
Sternlicht, M.D., Werb, Z., 2001. Annu. Rev. Cell Dev. Biol. 17, 463–516.
Woessner, J.F., 1998. The matrix metalloproteinase family. In: Parks, W.C., Mecham, R.P. (Eds.), Matrix Metalloproteinases. Academic Press, San Diego, pp. 1–14.
Riley, G.P., Harrall, R.L., Watson, P.G., Cawston, T.E., Hazleman, B.L., 1995. Eye 9, 703–718, Pt 6.
Caravan, P., Das, B., Dumas, S., Epstein, F.H., Helm, P.A., Jacques, V., Koerner, S., Kolodziej, A., Shen, L., Sun, W.C., Zhang, Z., 2007. Angew. Chem. Int. Ed. Engl. 46, 8171–8173.
Mueller, J., Gaertner, F.C., Blechert, B., Janssen, K.P., Essler, M., 2009. Mol. Cancer Res. 7, 1078–1085.
Pernasetti, F., Nickel, J., Clark, D., Baeuerle, P.A., Van Epps, D., Freimark, B., 2006. Int. J. Oncol. 29, 1371–1379.
Xu, J., Rodriguez, D., Kim, J.J., Brooks, P.C., 2000. Hybridoma 19, 375–385.
Chichester, C., Barrach, H.J., Chichester, A., Matoney, A., Srinivas, G.R., 1991. J. Immunol. Methods 140, 259–267.
Srinivas, G.R., Chichester, C.O., Barrach, H.J., Pillai, V., Matoney, A.L., 1994. Immunol. Investig. 23, 85–98.
Sapsford, K.E., Berti, L., Medintz, I.L., 2006. Angew. Chem. Int. Ed. Engl. 45, 4562–4589.
Novoselov, K.S., Geim, A.K., Morozov, S.V., Jiang, D., Zhang, Y., Dubonos, S.V., Grigorieva, I.V., Firsov, A.A., 2004. Science 306, 666–669.
Kumar, S., Ahlawat, W., Kumar, R., Dilbaghi, N., 2015. Biosens. Bioelectron. 70, 498–503.
Yang, W., Ratinac, K.R., Ringer, S.P., Thordarson, P., Gooding, J.J., Braet, F., 2010. Angew. Chem. Int. Ed. Engl. 49, 2114–2138.
Lu, C.H., Yang, H.H., Zhu, C.L., Chen, X., Chen, G.N., 2009. Angew. Chem. Int. Ed. Engl. 48, 4785–4787.
Jang, H., Kim, Y.K., Kwon, H.M., Yeo, W.S., Kim, D.E., Min, D.H., 2010. Angew. Chem. Int. Ed. Engl. 49, 5703–5707.
Yang, Q., Li, F., Huang, Y., Xu, H., Tang, L., Wang, L., Fan, C., 2013. Analyst 138, 2057–2060.
Feng, D., Zhang, Y., Feng, T., Shi, W., Li, X., Ma, H., 2011. Chem. Commun. 47, 10680–10682.
Lu, C.H., Li, J., Zhang, X.L., Zheng, A.X., Yang, H.H., Chen, X., Chen, G.N., 2011. Anal. Chem. 83, 7276–7282.
Bianying, F., Linjie, G., Lihua, W., Fan, L., Jianxin, L., Jimin, G., Chunhai, F., Qing, H., 2013. Anal. Chem. 85, 7732–7737.
Brodsky, B., Ramshaw, J.A., 1997. Matrix Biol. 15, 545–554.
Gao, L., Lian, C., Zhou, Y., Yan, L., Li, Q., Zhang, C., Chen, L., Chen, K., 2014. Biosens. Bioelectron. 60, 22–29.
Wang, A.Y., Mo, X., Chen, C.S., Yu, S.M., 2005. J. Am. Chem. Soc. 127, 4130–4131.
He, Y., Lin, Y., Tang, H., Pang, D., 2012. Nanoscale 4, 2054–2059.
Bhunia, S.K., Jana, N.R., 2011. ACS Appl. Mater. Interfaces 3, 3335–3341.
Song, E., Cheng, D., Song, Y., Jiang, M., Yu, J., Wang, Y., 2013. Biosens. Bioelectron. 47, 445–450.
Nandi, S., Routh, P., Layek, R.K., Nandi, A.K., 2012. Biomacromolecules 13, 3181–3188.
Wu, C., Zhou, Y., Miao, X., Ling, L., 2011. Analyst 136, 2106–2110.
Sabale, P.M., George, J.T., Srivatsan, S.G., 2014. Nanoscale 6, 10460–10469.
Liu, H., Wang, Y., Shen, A., Zhou, X., Hu, J., 2012. Talanta 93, 330–335.